JACS Au
AN OPEN ACCESS JOURNAL OF THE AMERICAN CHEMICAL SOCIETY

Open Access
This article is licensed under CC-BY-NC-ND 4.0

pubs.acs.org/jacsau
Article

Divergent Synthesis of Chiroptical Molecular Switches Based on 1,2-Diaxial Atropisomers

Tian-Jiao Han, Qiu-Le Yang, Jiaen Hu, Min-Can Wang, and Guang-Jian Mei*

Cite This: *JACS Au* 2024, 4, 4445−4454
Read Online

ACCESS | Metrics & More | Article Recommendations | Supporting Information

ABSTRACT: The development of chiroptical molecular switches for chiral sensing, data communication, optical displays, chiral logic gates, and asymmetric catalysis is currently a vibrant frontier of science and technology. Herein, we report a practical artificial dynamic system based on a 1,2-diaxial atropisomer. Organocatalytic parallel kinetic resolution allows the divergent synthesis of two sets of stereoisomers with vicinal C−C and N−N axes from the same racemic single-axis substrates. By simply varying the configuration of the single catalyst, all four stereoisomers are accessible. The successive conduction of covalent unlocking/locking and thermal-isomerization processes enables sequential switching between all four atropisomeric states with electronic circular dichroism signal reversal, providing an example of multistate chiroptical molecular switches.

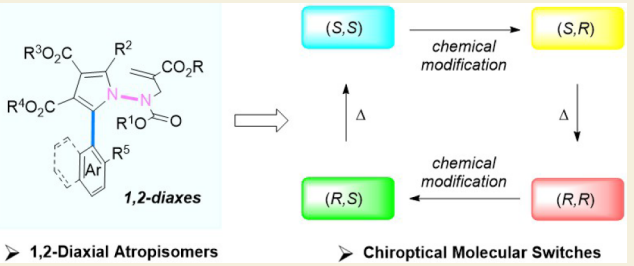

KEYWORDS: *molecular switch, chiroptical, 1, 2-diaxial atropisomer, parallel kinetic resolution, divergent synthesis*

INTRODUCTION

Chiroptical molecular switches refer to molecular systems whose chiral optical signals, including electronic circular dichroism (ECD), optical rotatory dispersion (ORD) and circularly polarized luminescence (CPL) signals, can be reversibly interchanged between two or more stable states under external stimuli.[1−4] Due to their unique nondestructive readout, fast response times, reproducibility and fatigue resistance, chiroptical molecular switches offer fascinating prospects in the fields of chiral sensing, optical displays, information storage, chiral logic gates, asymmetric catalysis and so on.[5] Therefore, the development of innovative artificial dynamic systems to fabricate efficient chiroptical molecular switches is a field of continuous interest.[6−15]

Over the past decade, significant progress has been made in the enantioselective synthesis of atropisomers, an important class of chiral molecules arising from restricted rotation around a single bond.[16−29] Biaryl-type atropisomers are a typical basis of molecular machines due to their rotatory mechanism (Figure 1A).[30−34] Distinct interconversion by rotation of the atropisomers, i.e., epimerization, is possible simply by chemical modification (CM) of the *ortho*-substituents. A fascinating class of monoaxial molecular machines, including switches, rotors and motors, have been artificially manufactured, and convert chemical energy into rotational motion around single bonds.[35−43] 1,2-Diaxial atropisomers represent a particular subtype with an intrinsic dynamic system of multiple states (Figure 1B). The rotation of both axes can produce four possible stereoisomers with individual chiroptical properties. At adjacent positions, the two axes can interact with each other due to steric effects, i.e., the stereochemistry of one axis can affect the rotation of the other axis. Controlling the interconversion between multiple states of a 1,2-diaxial system by external stimuli is potentially useful for chiroptical molecular devices. However, such fascinating applications have been greatly limited by the lack of atroposelective synthesis.[44,45] The difficulty of assembling vicinal stereoaxes with simultaneous enantio- and diastereocontrol poses a daunting challenge. To date, only a few successful approaches have been reported, including [2 + 2 + 2] cycloadditions of triynes,[46,47] arene-forming aldol condensations,[48,49] central-to-axial chirality conversions,[50,51] organocatalytic annulations,[52−54] and asymmetric C−H activations.[55−57] However, these protocols can only stereoselectively deliver the product of one of the four possible stereoisomers. In 2022, Moser and Sparr pioneered the stereodivergent synthesis of atropisomeric two-axis systems with moderate stereoselectivity.[58] Despite these achievements, the enantioselective synthesis, especially in a divergent manner,[59−63] of 1,2-diaxial atropisomers is still in its infancy. The chiroptical switching between conceivable stereoisomers of a 1,2-diaxial atropisomer has not yet been reported.

Recently, we accomplished the catalytic asymmetric synthesis of C−C and N−N atropisomers, and constructed a 1,2-diaxial

Received: August 25, 2024
Revised: September 26, 2024
Accepted: September 27, 2024
Published: October 14, 2024

© 2024 The Authors. Published by American Chemical Society

https://doi.org/10.1021/jacsau.4c00777
JACS Au 2024, 4, 4445−4454

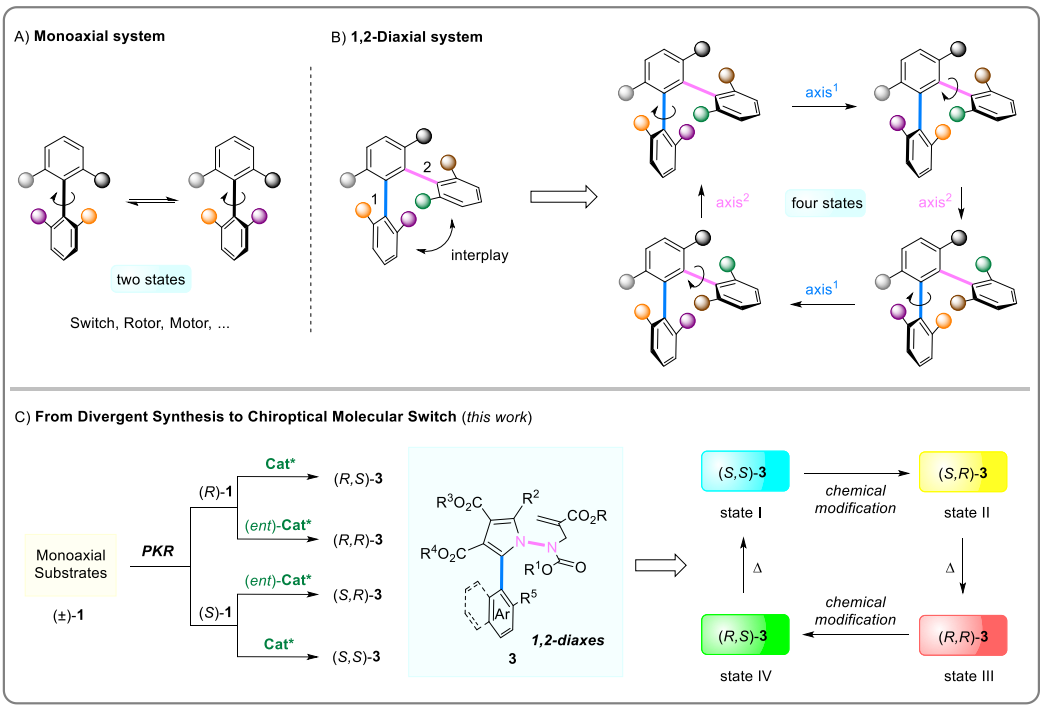

Figure 1. Divergent synthesis of 1,2-diaxial atropisomers as chiroptical molecular switches.

Table 1. Reaction Optimization[a]

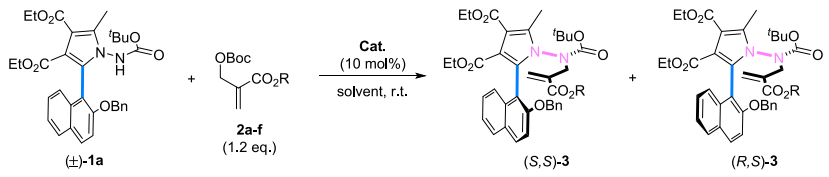

				(*S*,*S*)-3		(*R*,*S*)-3	
Entry	Cat.	Solvent	R (3)	Yield (%)[b]	*ee*(%)[c]	Yield (%)[b]	*ee*(%)[c]
1	**C1**	CH_2Cl_2	^{t}Bu (**3a**)	91 (**1.6**:1)	−60	91 (1.6:**1**)	−98
2	**C2**	CH_2Cl_2	^{t}Bu (**3a**)	83 (**1.2**:1)	79	83 (1.2:**1**)	98
3	**C3**	CH_2Cl_2	^{t}Bu (**3a**)	93 (**1.5**:1)	−65	93 (1.5:**1**)	−98
4	**C4**	CH_2Cl_2	^{t}Bu (**3a**)	95 (**1.2**:1)	80	95 (1.2:**1**)	98
5	**C5**	CH_2Cl_2	^{t}Bu (**3a**)	80 (**1**:1)	60	80 (1:**1**)	94
6	**C6**	CH_2Cl_2	^{t}Bu (**3a**)	87 (**1.8**:1)	−45	87 (1.8:**1**)	−97
7	**C4**	toluene	^{t}Bu (**3a**)	83 (**1.5**:1)	58	83 (1.5:**1**)	96
8	**C4**	CH_3CN	^{t}Bu (**3a**)	85 (**1.4**:1)	56	85 (1.4:**1**)	84
9	**C4**	THF	^{t}Bu (**3a**)	80 (**2.2**:1)	26	80 (2.2:**1**)	74
10	**C4**	CH_2Cl_2	Me (**3b**)	98 (**1.1**:1)	90	98 (1.1:**1**)	98
11	**C4**	CH_2Cl_2	Et (**3c**)	97 (**1.1**:1)	88	97 (1.1:**1**)	96
12	**C4**	CH_2Cl_2	Bn (**3d**)	94 (**1.3**:1)	81	94 (1.3:**1**)	94
13	**C4**	CH_2Cl_2	^{n}Bu (**3e**)	92 (**1.3**:1)	81	92 (1.3:**1**)	96
14	**C4**	CH_2Cl_2	^{i}Bu (**3f**)	94 (**1.3**:1)	81	94 (1.3:**1**)	96

[a]Reaction conditions: **1a** (0.1 mmol), **2** (0.12 mmol), and **Cat.** (10 mol %) in the solvent specified (1 mL) at room temperature (r.t.) for 12 h. [b]Isolated yields, dr was determined by crude ^{1}H NMR. [c]Determined by chiral HPLC analysis.

hybrid via dynamic kinetic resolution (DKR).[64−66] However, the previous system contained a labile C−C axis that rotated freely at ambient temperature and therefore did not exhibit the characteristic stimulus response of a molecular machine. Herein, we report the divergent synthesis of stable 1,2-diaxial atropisomers via parallel kinetic resolution (PKR) (Figure

https://doi.org/10.1021/jacsau.4c00777
JACS Au 2024, 4, 4445−4454

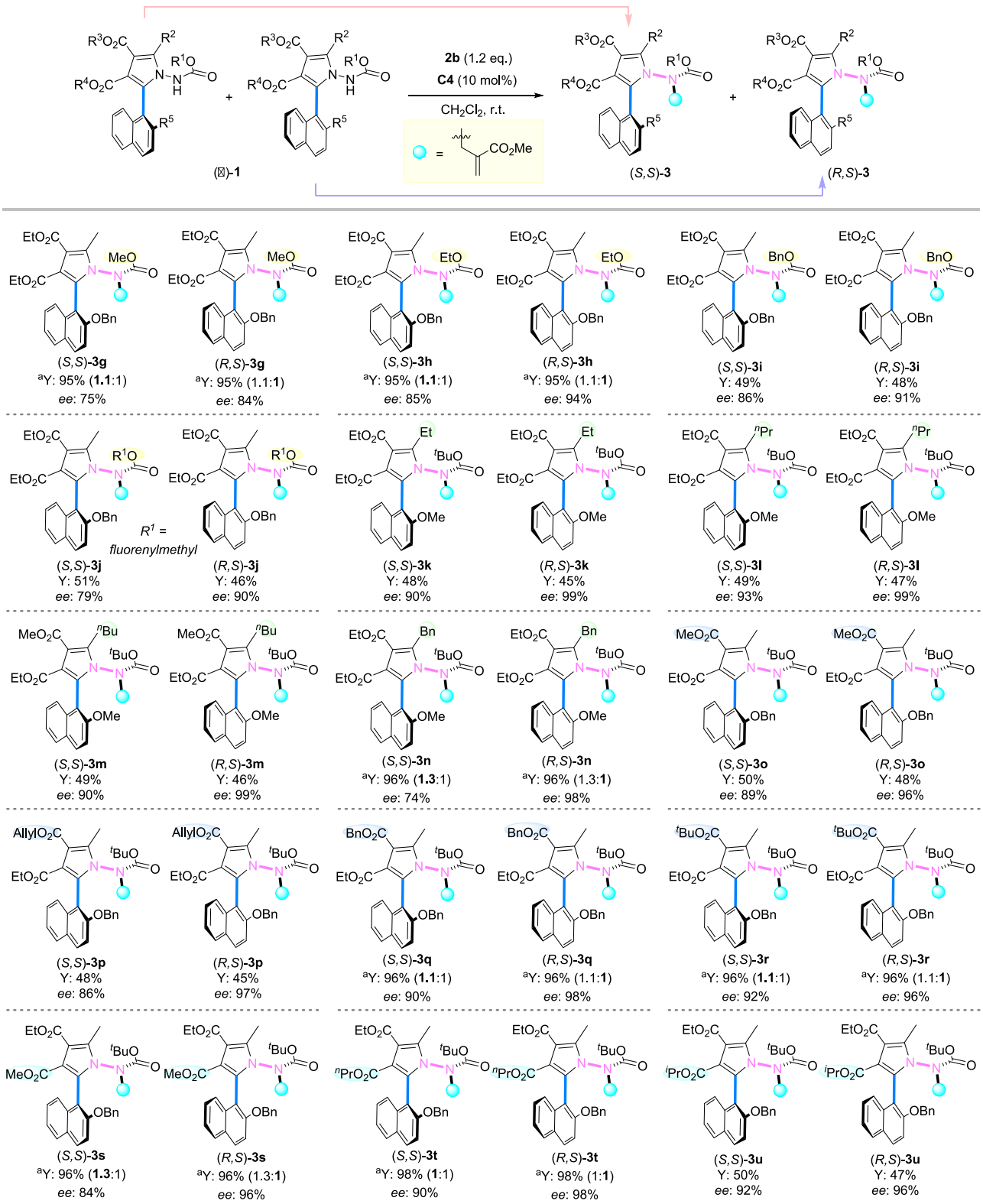

Figure 2. Scope of the upper pyrrole motif. Reaction conditions: **1** (0.1 mmol), **2b** (0.12 mmol), and **C4** (10 mol %) in CH_2Cl_2 (1 mL) at r.t. for 6 h. Isolated yields. The *ee* values were determined by HPLC analysis on a chiral stationary phase. [a] signifies nonseparable isomers.

1C).[67−74] The reaction features simple operation, mild conditions, broad scope, and good enantioselectivity. All four possible stereoisomers with vicinal C−C and N−N axes are accessible by simply varying the configuration of the single catalyst. More importantly, the successive conduction of covalent unlocking/locking and thermal-isomerization processes allows sequential switching between the all four atropisomeric states, providing a new example of multistate chiroptical molecular switches.

https://doi.org/10.1021/jacsau.4c00777
JACS Au 2024, 4, 4445−4454

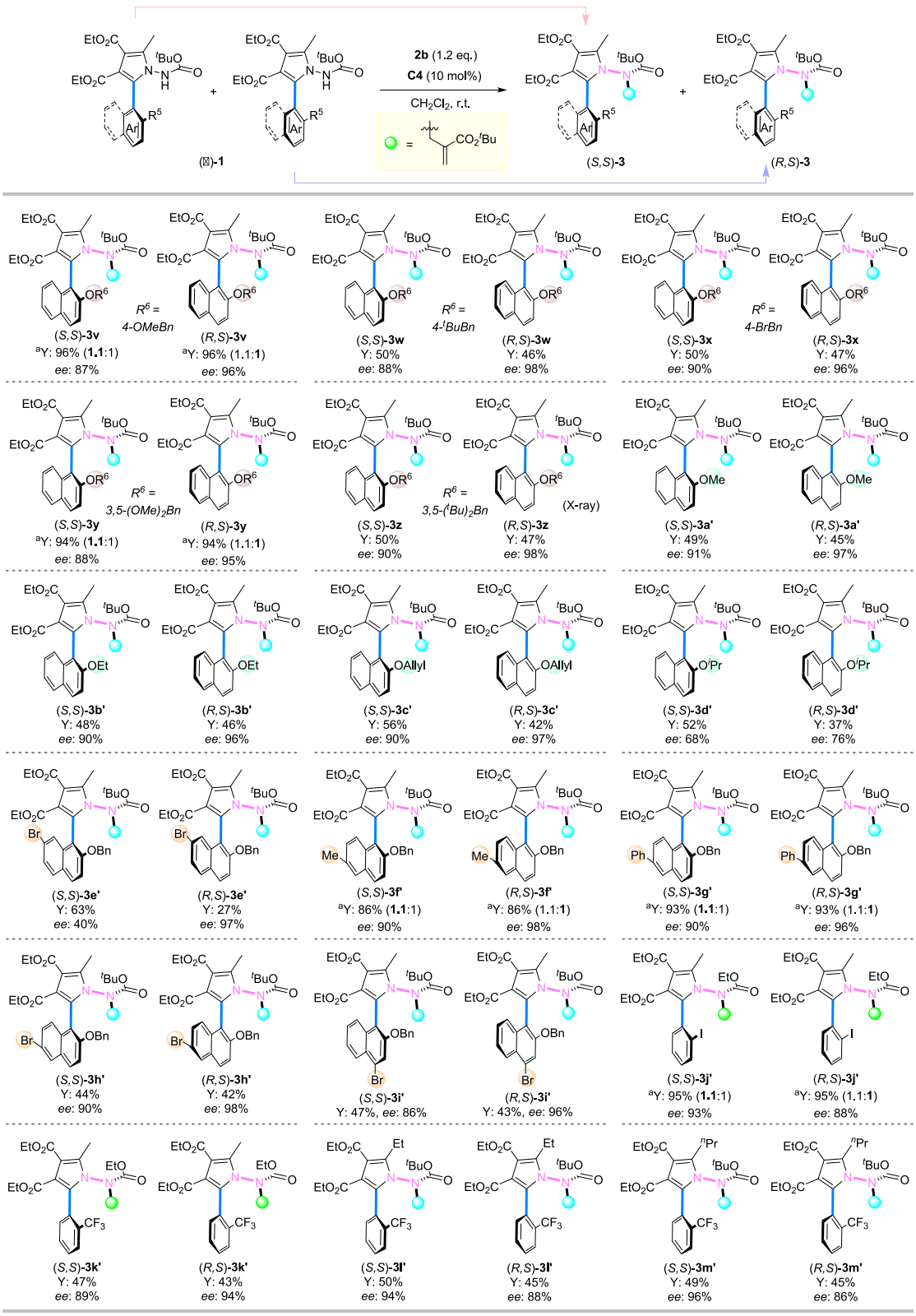

Figure 3. Scope of the lower aromatic motif. Reaction conditions: **1** (0.1 mmol), **2b** (0.12 mmol), and **C4** (10 mol %) in CH_2Cl_2 (1 mL) at r.t. for 6 h. Isolated yields. The *ee* values were determined by HPLC analysis on a chiral stationary phase. [a] signifies nonseparable isomers.

RESULTS AND DISCUSSION

We commenced this work by preparing enantioenriched 1,2-diaxial atropisomers. We used the asymmetric *N*-allylation of **1a** with the Morita−Baylis−Hillman (MBH)[75−77] adduct **2a** in our model study (Table 1). Under quinine catalysis, the PKR of (±)-**1a** with **2a** (1.2 equiv) occurred, affording two diastereoisomers of **3a** in 91% yield with a 1.6:1 ratio (entry 1). The *ee* value of the major stereoisomer (*R*,*R*)-**3a** was moderate (60%), while that of the minor one (*S*,*R*)-**3a** was excellent (98%). Moreover, the use of the *pseudo*-enantiomer catalyst quinidine

https://doi.org/10.1021/jacsau.4c00777
JACS Au 2024, 4, 4445−4454

enabled the divergent synthesis of the other two stereoisomers, (*S*,*S*)-**3a** and (*R*,*S*)-**3a** (entry 2). Various cinchona bases were then screened (entries 3−6), and the results indicated that hydroquinidine **C4** was the best choice (entry 4). We evaluated the effect of the solvent and found that dichloromethane was the optimal solvent (entry 4 vs 7−9). The screening of other conditions, such as reaction temperature and additives, failed to provide further improvement (see Supporting Information for details). Considering that the ester group of MBH adducts may have some influence on the enantioselectivity, various MBH adducts were tested (entries 10−14). Although they were all compatible, MBH adduct **2b** with smaller methyl ester groups provided the best results (entry 10).

With the best conditions, we examined the substrate generality of this PKR reaction. As shown in Figure 2, this PKR was applicable to a wide range of racemic atropisomers **1** with a substituted pyrrole motif. Considering the steric effect of the *ortho*-substituent, the tolerance of the carbamate group (−NCO_2R^1) was first evaluated. As expected, when sterically hindered −$NCO_2{}^t$Bu (**3b**) was replaced with the less hindered −NCO_2Me (**3g**), −NCO_2Et (**3h**), −NCO_2Bn (**3i**), or −N-Fmoc (**3j**), the enantioselectivity decreased. However, the *ortho*-substituent R^2 had a delicate influence. While the substituents ethyl (**3k**), *n*-propyl (**3l**), and *n*-butyl (**3m**) were well tolerated, benzyl (**3n**) was only beneficial for the formation of minor isomer. Due to the long distance from both the C−C and N−N axes, the ester group −CO_2R^3 had little influence on the reaction. Therefore, products **3o**−**r** were obtained with excellent enantioselectivities. With respect to the ester group −CO_2R^4, the steric effect of the bulky groups facilitated high enantiocontrol (**3s**−**u**).

Next, we focused on the lower aromatic motif (Figure 3). The variation of the protecting groups R^6 showed that the substituted benzyl groups were all compatible (**3v**−**z**). Alkyl groups such as methyl (**3a′**), ethyl (**3b′**), and allyl (**3c′**) groups were also well tolerated, delivering the corresponding diastereoisomers in good yields with excellent *ee* values. However, a sterically hindered protecting group (**3d′**) was not suitable because it significantly decreased the enantioselectivity. Moreover, the position of the substituent on the naphthalene ring had some impact on the enantioselectivity. For instance, bromo groups at the C4- (**3i′**) or C6-position (**3h′**) afforded higher stereoselectivities than those at the C7-position (**3e′**). However, the type of substituent had no effect on this reaction. Electron-donating and electron-withdrawing groups afforded the same good yields and excellent enantioselectivities (**3f′**−**i′**). Notably, changing the naphthalene ring to a benzene ring was also feasible. Under standard conditions, the 1,2-diaxial atropisomers **3j′**−**m′** bearing a less hindered C−C axis were obtained with consistently excellent enantioselectivity.

To examine the practicality of this method, all four stereoisomers of **3z** were prepared. As shown in Figure 4, standard PKR conditions with catalyst **C4** allowed the formation of two stereoisomers (*S*,*S*)-**3z** and (*R*,*S*)-**3z** in good yields with excellent enantioselectivities. In general, by using the enantiomer of **C4**, the other two stereoisomers should be obtained in similar excellent results. However, only the *pseudo*-enantiomer **C3**, not its enantiomer, is readily available. With this nonideal alternative, the other two stereoisomers were obtained, despite the moderate enantioselectivity of (*R*,*R*)-**3z**. The absolute configuration of the product (*R*,*S*)-**3z** was assigned based on X-ray crystallographic analysis, and the absolute configurations of the other products were assigned by analogy.[78]

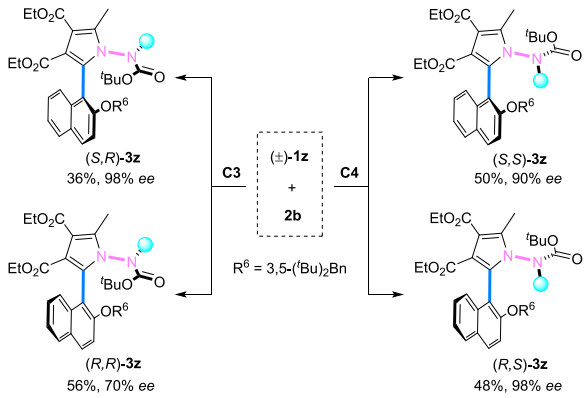

Figure 4. Access to all four stereoisomers of **3z**.

In addition, derivatization and control experiments were conducted to explore the synthetic utility and mechanism of this protocol, respectively (see the SI for details).

In the design of a 1,2-diaxial chiroptical switch, we use thermal-isomerization and chemical modification to program the chirality of the two axes, and six distinct steps, as depicted in Figure 5A. The switching cycle starts from the state 1. By the unlocking/locking process of one axis (pink), we could facilitate the movement of the 1,2-diaxial system from state 1 to state 3, via the configurationally labile intermediates in state 2. The use of an external chiral catalyst in the locking process will result in a predominance of the kinetic atropdiastereomer (state 3), and the thermal-isomerization of the other axis (blue) leads to a more stable state 4 and a complete inversion of both axial chiralities. Similarly, the remaining half cycle can be achieved using the same sequence of steps, and the switch returns to its initial conformation. There are two fundamental requirements for achieving the switching cycle: (1) the blue axis of state 2 or state 5 should have a sufficiently high rotational barrier to survive in the locking process; (2) to prevent direct reversal and racemization during thermal-isomerization, the rotation barrier of the pink axis must be much greater than that of the blue axis. Therefore, we studied the rotational barriers of several representative compounds synthesized above to determine the best 1,2-diaxial basis for chiroptical switching (Figure 5B). The racemization experiments (see Supporting Information for details) indicated that the barrier to conformer rotation around the C−C axis in **1a** and **1k'** is sufficiently high, but very low in **1j'**. We then investigated the 1,2-diaxial systems derived from **1a** and **1k'**. In naphthyl **3h'**, the rotational barrier of the C−C axis is much greater than that of the N−N axis, which will lead to direct reverse switching of the N−N axis during thermal-isomerization. This unfavorable effect was reversed for phenyl **3k'**−**m'**, and as the steric hindrance of the *ortho*-substituents on pyrrole increased, the rotational barrier difference between the two axes increased. With a sufficient barrier difference (≥4 kcal/mol), **3l'** or **3m'** can be selected as the optimal 1,2-diaxial system.

Finally, the switching process was investigated (Figure 6A). The first half cycle involves conformational inversion from (*S*,*S*)-**3l'** to (*R*,*R*)-**3l'**. Selective deprotection of the allyl group with NaOH allowed the N−N axis to be "unlocked", affording (*S*)-**1l'** in 93% yield. The slight decrease in the *ee* value is due to racemization caused by the rotation of the C−C axis. Asymmetric catalysis is a key step that ensures the formation of a thermodynamically less favored (*S*,*R*)-isomer. Using the organocatalytic PKR protocol developed above, the N−N axis was chemically "locked" to give the reversal allylation product

https://doi.org/10.1021/jacsau.4c00777
JACS Au 2024, 4, 4445−4454

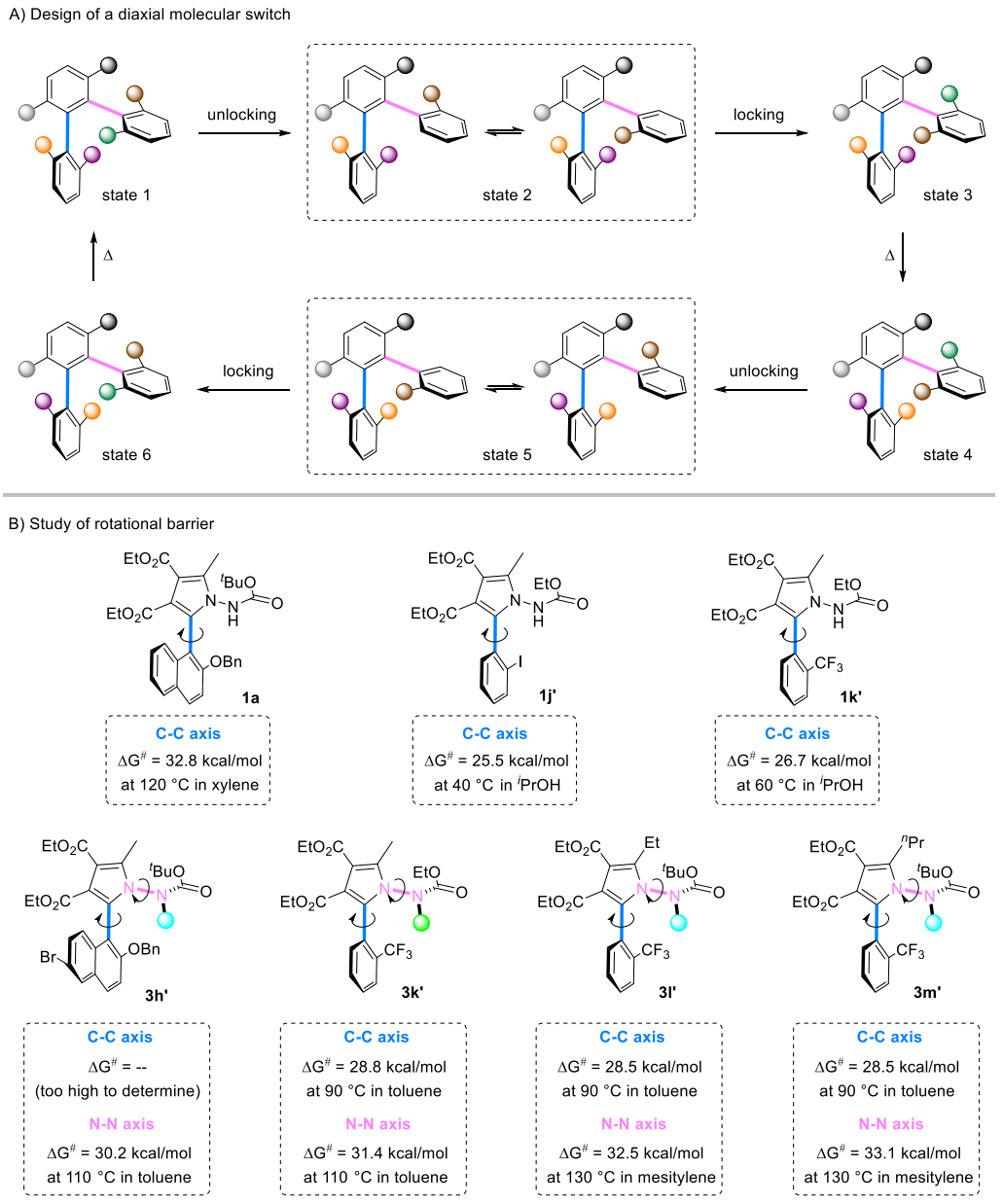

Figure 5. Design of a diaxial molecular switch and study of rotational barrier.

(*S,R*)-**3l'** and restore the enantioselectivity to an excellent level (97% *ee*). Subsequent heating at 60 °C in isopropanol led to the isomerization of the kinetic product to the thermodynamic product (*R,R*)-**3l'** through rotation of the N−N axis. The remaining half cycle was accomplished following the same principle. Through the above 6 steps, sequential switching between the four atropisomers of **3l'** was achieved. Regarding naphthyl system, the high rotational barrier of the C−C axis caused a direct reverse rotation of the N−N axis during thermal-isomerization, resulting in a switch between the two atropisomers of **3b** (Figure 6B). To probe the chiroptical properties and further understand the different steps of the cycles, we used ECD spectroscopy. As shown in Figure 6C, on the corresponding ECDs each state was clearly distinguishable. Consequently, the mode of write-in via covalent-modification and readout by chiroptical made this 1,2-diaxial system a new type of multistate chiroptical molecular switch.

CONCLUSION

In conclusion, we have developed a novel 1,2-diaxial system for chiroptical molecular switches. Organocatalytic parallel kinetic resolution allows simultaneous enantio-control over the vicinal C−C axis and N−N axis. Under mild conditions, two sets of 1,2-diaxial atropisomers with good to excellent enantioselectivities were readily prepared from the same racemic single-axis substrates. Notably, all four stereoisomers are accessible by simply varying the configuration of the single catalyst. The successive covalent unlocking/locking and thermal-isomerization processes enable sequential switching between all four atropisomeric states with electronic circular dichroism signal reversal, providing a new example of multistate chiroptical molecular switches. Further application of this 1,2-diaxial system in molecular rotors is ongoing in our laboratory and will be reported in due course.

https://doi.org/10.1021/jacsau.4c00777
JACS Au 2024, 4, 4445−4454

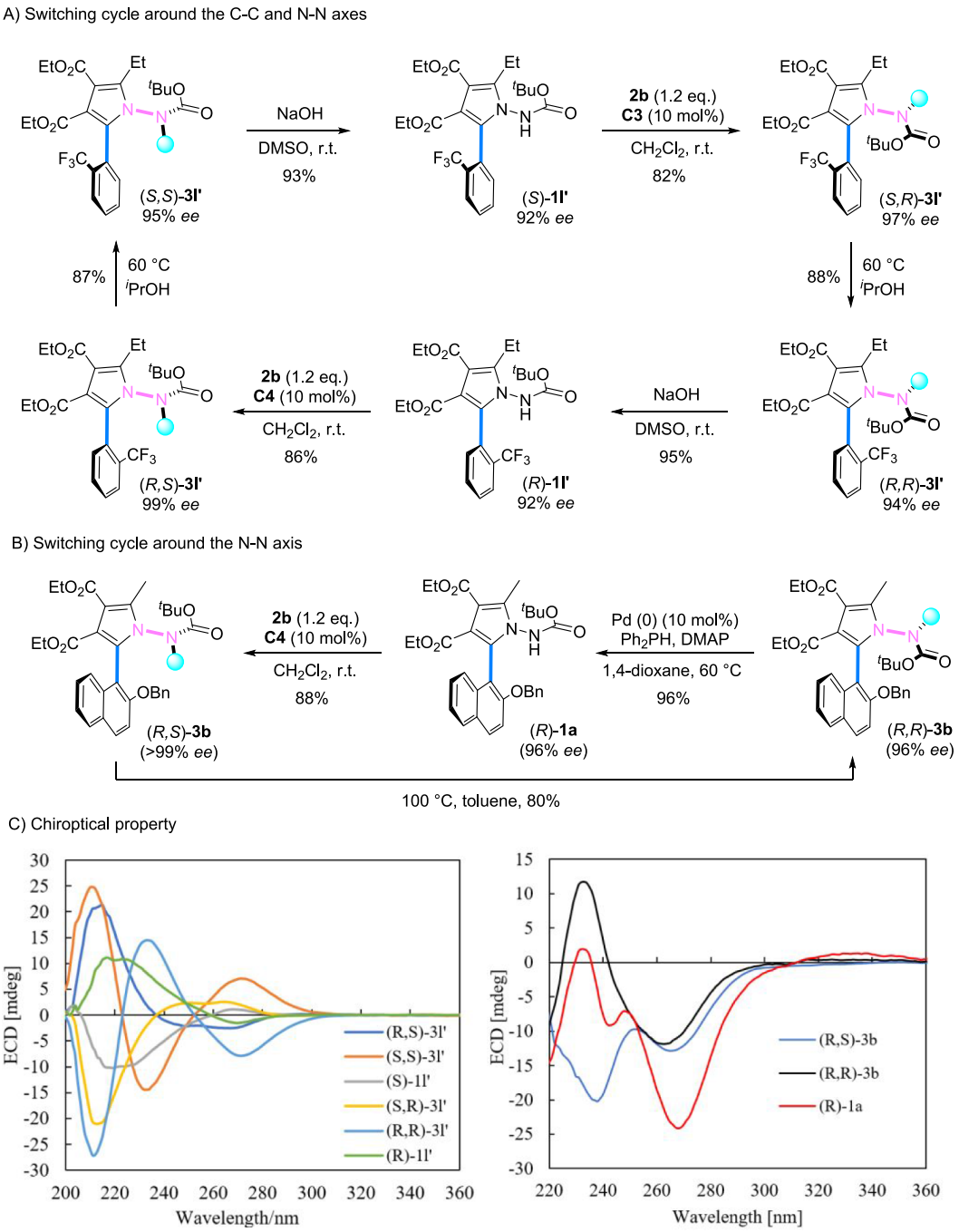

Figure 6. Chiroptical switching. ECD (5×10^{-5} M) spectra in CH_3OH.

METHODS

General Procedure of PKR

Racemic axial chiral compounds **1** (0.10 mmol), MBH carbonic esters **2** (0.12 mmol) were dissolved in CH_2Cl_2 (1 mL), and **C4** (10 mol %) was added. The reaction mixture was stirred for 6 h at room temperature. The solvent was removed in vacuo and the crude product was separated by flash column chromatography on silica gel (DCM/acetone = 50:1) to afford the products (*S*,*S*)-**3** and (*R*,*S*)-**3**.

ASSOCIATED CONTENT

Supporting Information

The Supporting Information is available free of charge at https://pubs.acs.org/doi/10.1021/jacsau.4c00777.

Experimental procedures, characterization data for all the products, computational data, energetics, and Cartesian coordinates for all calculated species (PDF)

Crystallographic data for compound (*R*,*S*)-**3z** (CIF)

AUTHOR INFORMATION

Corresponding Author

Guang-Jian Mei − *College of Chemistry, Zhengzhou University, Zhengzhou 450001, China; Pingyuan Laboratory*

https://doi.org/10.1021/jacsau.4c00777
JACS Au 2024, 4, 4445−4454

(Zhengzhou University), Zhengzhou 450001, China; orcid.org/0000-0002-8248-2327; Email: meigj@zzu.edu.cn

Authors

Tian-Jiao Han − *College of Chemistry, Zhengzhou University, Zhengzhou 450001, China*

Qiu-Le Yang − *College of Chemistry, Zhengzhou University, Zhengzhou 450001, China*

Jiaen Hu − *College of Chemistry, Zhengzhou University, Zhengzhou 450001, China*

Min-Can Wang − *College of Chemistry, Zhengzhou University, Zhengzhou 450001, China;* orcid.org/0000-0002-3817-3607

Complete contact information is available at: https://pubs.acs.org/10.1021/jacsau.4c00777

Notes

The authors declare no competing financial interest.

■ ACKNOWLEDGMENTS

Financial supports from National Natural Science Foundation of China (22371265) and Natural Science Foundation of Henan Province (222300420084) are gratefully acknowledged.

■ REFERENCES

(1) Feringa, B. L.; van Delden, R. A.; Koumura, N.; Geertsema, E. M. Chiroptical Molecular Switches. *Chem. Rev.* **2000**, *100* (5), 1789−1816.
(2) Canary, J. W. Redox-triggered chiroptical molecular switches. *Chem. Soc. Rev.* **2009**, *38* (3), 747.
(3) Canary, J. W.; Mortezaei, S.; Liang, J. Transition metal-based chiroptical switches for nanoscale electronics and sensors. *Coord. Chem. Rev.* **2010**, *254* (19−20), 2249−2266.
(4) Zhang, L.; Wang, H.-X.; Li, S.; Liu, M. Supramolecular chiroptical switches. *Chem. Soc. Rev.* **2020**, *49* (24), 9095−9120.
(5) Brandt, J. R.; Salerno, F.; Fuchter, M. J. The added value of small-molecule chirality in technological applications. *Nat. Rev. Chem.* **2017**, *1* (6), 0045.
(6) Feringa, B. L.; Jager, W. F.; De Lange, B.; Meijer, E. W. Chiroptical molecular switch. *J. Am. Chem. Soc.* **1991**, *113* (14), 5468−5470.
(7) Tietze, L. F.; Düfert, A.; Lotz, F.; Sölter, L.; Oum, K.; Lenzer, T.; Beck, T.; Herbst-Irmer, R. Synthesis of Chiroptical Molecular Switches by Pd-Catalyzed Domino Reactions. *J. Am. Chem. Soc.* **2009**, *131* (49), 17879−17884.
(8) Takaishi, K.; Yasui, M.; Ema, T. Binaphthyl−Bipyridyl Cyclic Dyads as a Chiroptical Switch. *J. Am. Chem. Soc.* **2018**, *140* (16), 5334−5338.
(9) Isla, H.; Saleh, N.; Ou-Yang, J.-K.; Dhbaibi, K.; Jean, M.; Dziurka, M.; Favereau, L.; Vanthuyne, N.; Toupet, L.; Jamoussi, B.; Srebro-Hooper, M.; Crassous, J. Bis-4-aza[6]helicene: A Bis-helicenic 2,2′-Bipyridine with Chemically Triggered Chiroptical Switching Activity. *J. Org. Chem.* **2019**, *84* (9), 5383−5393.
(10) Tong, S.; Li, J.-T.; Liang, D.-D.; Zhang, Y.-E.; Feng, Q.-Y.; Zhang, X.; Zhu, J.; Wang, M.-X. Catalytic Enantioselective Synthesis and Switchable Chiroptical Property of Inherently Chiral Macrocycles. *J. Am. Chem. Soc.* **2020**, *142* (34), 14432−14436.
(11) Yao, J.; Wu, W.; Xiao, C.; Su, D.; Zhong, Z.; Mori, T.; Yang, C. Overtemperature-protection intelligent molecular chiroptical photoswitches. *Nat. Commun.* **2021**, *12* (1), 2600.
(12) Yen-Pon, E.; Buttard, F.; Frédéric, L.; Thuéry, P.; Taran, F.; Pieters, G.; Champagne, P. A.; Audisio, D. Heterohelicenes through 1,3-Dipolar Cycloaddition of Sydnones with Arynes: Synthesis, Origins of Selectivity, and Application to pH-Triggered Chiroptical Switch with CPL Sign Reversal. *JACS Au* **2021**, *1* (6), 807−818.
(13) Han, Z.; Si, Y.; Dong, X.-Y.; Hu, J.-H.; Zhang, C.; Zhao, X.-H.; Yuan, J.-W.; Wang, Y.; Zang, S.-Q. Smart Reversible Transformations between Chiral Superstructures of Copper Clusters for Optical and Chiroptical Switching. *J. Am. Chem. Soc.* **2023**, *145* (11), 6166−6176.
(14) Li, J.; Cui, Y.; Lu, Y.-L.; Zhang, Y.; Zhang, K.; Gu, C.; Wang, K.; Liang, Y.; Liu, C.-S. Programmable supramolecular chirality in non-equilibrium systems affording a multistate chiroptical switch. *Nat. Commun.* **2023**, *14* (1), 5030.
(15) Sheng, J.; Danowski, W.; Crespi, S.; Guinart, A.; Chen, X.; Stähler, C.; Feringa, B. L. Designing P-type bi-stable overcrowded alkene-based chiroptical photoswitches. *Chem. Sci.* **2023**, *14* (16), 4328−4336.
(16) Wu, Y.-J.; Liao, G.; Shi, B.-F. Stereoselective construction of atropisomers featuring a C−N chiral axis. *Green Synth. Catal.* **2022**, *3* (2), 117−136.
(17) Mei, G.-J.; Koay, W. L.; Guan, C.-Y.; Lu, Y. Atropisomers beyond the C−C axial chirality: Advances in catalytic asymmetric synthesis. *Chem* **2022**, *8* (7), 1855−1893.
(18) Cheng, J. K.; Xiang, S. H.; Tan, B. Organocatalytic Enantioselective Synthesis of Axially Chiral Molecules: Development of Strategies and Skeletons. *Acc. Chem. Res.* **2022**, *55* (20), 2920−2937.
(19) Liu, C. X.; Zhang, W. W.; Yin, S. Y.; Gu, Q.; You, S. L. Synthesis of Atropisomers by Transition-Metal-Catalyzed Asymmetric C-H Functionalization Reactions. *J. Am. Chem. Soc.* **2021**, *143* (35), 14025−14040.
(20) Da, B. C.; Xiang, S. H.; Li, S.; Tan, B. Chiral Phosphoric Acid Catalyzed Asymmetric Synthesis of Axially Chiral Compounds. *Chin. J. Chem.* **2021**, *39* (7), 1787−1796.
(21) Cheng, J. K.; Xiang, S. H.; Li, S.; Ye, L.; Tan, B. Recent Advances in Catalytic Asymmetric Construction of Atropisomers. *Chem. Rev.* **2021**, *121* (8), 4805−4902.
(22) Wang, Y. B.; Tan, B. Construction of Axially Chiral Compounds via Asymmetric Organocatalysis. *Acc. Chem. Res.* **2018**, *51* (2), 534−547.
(23) Zhang, Z.-J.; Simon, M. M.; Yu, S.; Li, S.-W.; Chen, X.; Cattani, S.; Hong, X.; Ackermann, L. Nickel-Catalyzed Atroposelective C−H Alkylation Enabled by Bimetallic Catalysis with Air-Stable Heteroatom-Substituted Secondary Phosphine Oxide Preligands. *J. Am. Chem. Soc.* **2024**, *146* (13), 9172−9180.
(24) Yang, Y.; Wu, C.; Xing, J.; Dou, X. Developing Biarylhemiboronic Esters for Biaryl Atropisomer Synthesis via Dynamic Kinetic Atroposelective Suzuki−Miyaura Cross-Coupling. *J. Am. Chem. Soc.* **2024**, *146* (9), 6283−6293.
(25) Wu, M.; Chen, Y.-W.; Lu, Q.; Wang, Y.-B.; Cheng, J. K.; Yu, P.; Tan, B. Organocatalytic Si−CAryl Bond Functionalization-Enabled Atroposelective Synthesis of Axially Chiral Biaryl Siloxanes. *J. Am. Chem. Soc.* **2023**, *145* (37), 20646−20654.
(26) Li, J.-J.; Zhao, J.-H.; Shen, H.-C.; Wu, K.; Kuang, X.; Wang, P.; Yu, J.-Q. Atroposelective remote meta-C−H activation. *Chem.* **2023**, *9* (6), 1452−1463.
(27) Jiang, P.-Y.; Wu, S.; Wang, G. J.; Xiang, S. H.; Tan, B. Synthesis of Axially Chiral QUINAP Derivatives by Ketone-Catalyzed Enantioselective Oxidation. *Angew. Chem., Int. Ed.* **2023**, *62* (40), No. e202309272.
(28) Da, B.-C.; Wang, Y. B.; Cheng, J. K.; Xiang, S. H.; Tan, B. Organocatalytic Atroposelective Cross-Coupling of 1-Azonaphthalenes and 2-Naphthols. *Angew. Chem., Int. Ed.* **2023**, *62* (25), No. e202303128.
(29) Chen, Y.-H.; Duan, M.; Lin, S.-L.; Liu, Y.-W.; Cheng, J. K.; Xiang, S.-H.; Yu, P.; Houk, K. N.; Tan, B. Organocatalytic aromatization-promoted umpolung reaction of imines. *Nat. Chem.* **2024**, *16* (3), 408−416.
(30) Mayer, L. C.; Heitsch, S.; Trapp, O. Nonlinear Effects in Asymmetric Catalysis by Design: Concept, Synthesis, and Applications. *Acc. Chem. Res.* **2022**, *55* (23), 3345−3361.
(31) Scholtes, J. F.; Trapp, O. Inducing Enantioselectivity in a Dynamic Catalyst by Supramolecular Interlocking. *Angew. Chem., Int. Ed.* **2019**, *58* (19), 6306−6310.
(32) Storch, G.; Trapp, O. By-design enantioselective self-amplification based on non-covalent product−catalyst interactions. *Nat. Chem.* **2017**, *9* (2), 179−187.

(33) Storch, G.; Trapp, O. Temperature-Controlled Bidirectional Enantioselectivity in a Dynamic Catalyst for Asymmetric Hydrogenation. *Angew. Chem., Int. Ed.* **2015**, *54* (12), 3580−3586.
(34) Maier, F.; Trapp, O. Selector-Induced Dynamic Deracemization of a Selectand-Modified Tropos BIPHEPO-Ligand: Application in the Organocatalyzed Asymmetric Double-Aldol-Reaction. *Angew. Chem., Int. Ed.* **2014**, *53* (33), 8756−8760.
(35) Mondal, A.; Toyoda, R.; Costil, R.; Feringa, B. L. Chemically Driven Rotatory Molecular Machines. *Angew. Chem., Int. Ed.* **2022**, *61* (40), No. e202206631.
(36) Sahoo, D.; Benny, R.; Ks, N. K.; De, S. Stimuli-Responsive Chiroptical Switching. *ChemPluschem* **2022**, *87* (2), No. e202100322.
(37) Zwick, P.; Troncossi, A.; Borsley, S.; Vitorica-Yrezabal, I. J.; Leigh, D. A. Stepwise Operation of a Molecular Rotary Motor Driven by an Appel Reaction. *J. Am. Chem. Soc.* **2024**, *146* (7), 4467−4472.
(38) Borsley, S.; Kreidt, E.; Leigh, D. A.; Roberts, B. M. W. Autonomous fuelled directional rotation about a covalent single bond. *Nature* **2022**, *604* (7904), 80−85.
(39) Zhang, Y.; Chang, Z.; Zhao, H.; Crespi, S.; Feringa, B. L.; Zhao, D. A Chemically Driven Rotary Molecular Motor Based on Reversible Lactone Formation with Perfect Unidirectionality. *Chem* **2020**, *6* (9), 2420−2429.
(40) Collins, B. S. L.; Kistemaker, J. C. M.; Otten, E.; Feringa, B. L. A chemically powered unidirectional rotary molecular motor based on a palladium redox cycle. *Nat. Chem.* **2016**, *8* (9), 860−866.
(41) Chong, Y. S.; Dial, B. E.; Burns, W. G.; Shimizu, K. D. Covalent locking and unlocking of an atropisomeric molecular switch. *Chem. Commun.* **2012**, *48* (9), 1296−1298.
(42) Fletcher, S. P.; Dumur, F.; Pollard, M. M.; Feringa, B. L. A Reversible, Unidirectional Molecular Rotary Motor Driven by Chemical Energy. *Science* **2005**, *310* (5745), 80−82.
(43) Kelly, T. R.; De Silva, H.; Silva, R. A. Unidirectional rotary motion in a molecular system. *Nature* **1999**, *401* (6749), 150−152.
(44) Zhang, H.-H.; Li, T. Z.; Liu, S. J.; Shi, F. Catalytic Asymmetric Synthesis of Atropisomers Bearing Multiple Chiral Elements: An Emerging Field. *Angew. Chem., Int. Ed.* **2024**, *63* (3), No. e202311053.
(45) Bao, X.; Rodriguez, J.; Bonne, D. Enantioselective Synthesis of Atropisomers with Multiple Stereogenic Axes. *Angew. Chem., Int. Ed.* **2020**, *59* (31), 12623−12634.
(46) Oppenheimer, J.; Hsung, R. P.; Figueroa, R.; Johnson, W. L. Stereochemical Control of Both C−C and C−N Axial Chirality in the Synthesis of Chiral N,O-Biaryls. *Org. Lett.* **2007**, *9* (20), 3969−3972.
(47) Shibata, T.; Tsuchikama, K.; Otsuka, M. Enantioselective intramolecular [2 + 2+2] cycloaddition of triynes for the synthesis of atropisomeric chiral ortho-diarylbenzene derivatives. *Tetrahedron* **2006**, *17* (4), 614−619.
(48) Lotter, D.; Neuburger, M.; Rickhaus, M.; Häussinger, D.; Sparr, C. Stereoselective Arene-Forming Aldol Condensation: Synthesis of Configurationally Stable Oligo-1,2-naphthylenes. *Angew. Chem., Int. Ed.* **2016**, *55* (8), 2920−2923.
(49) Lotter, D.; Castrogiovanni, A.; Neuburger, M.; Sparr, C. Catalyst-Controlled Stereodivergent Synthesis of Atropisomeric Multiaxis Systems. *ACS Cent. Sci.* **2018**, *4* (5), 656−660.
(50) Zhang, X.-L.; Gu, J.; Cui, W. H.; Ye, Z.; Yi, W.; Zhang, Q.; He, Y. Stepwise Asymmetric Allylic Substitution-Isomerization Enabled Mimetic Synthesis of Axially Chiral B,N-Heterocycles. *Angew. Chem., Int. Ed.* **2022**, *61*, No. e202210456.
(51) Hu, Y. L.; Wang, Z.; Yang, H.; Chen, J.; Wu, Z. B.; Lei, Y.; Zhou, L. Conversion of two stereocenters to one or two chiral axes: atroposelective synthesis of 2,3-diarylbenzoindoles. *Chem. Sci.* **2019**, *10* (28), 6777−6784.
(52) Zhang, S. C.; Liu, S. P.; Wang, X.; Wang, S. J.; Yang, H.; Li, L.; Yang, B. M.; Wong, M. W.; Zhao, Y.; Lu, S. C. Enantioselective Access to Triaryl-2-pyrones with Monoaxial or Contiguous C-C Diaxes via Oxidative NHC Catalysis. *ACS Catal.* **2023**, *13*, 2565−2575.
(53) Zhang, S.; Wang, X.; Han, L. L.; Li, J.; Liang, Z.; Wei, D.; Du, D. Atroposelective Synthesis of Triaryl α-Pyranones with 1,2-Diaxes by N-Heterocyclic Carbene Organocatalysis. *Angew. Chem., Int. Ed.* **2022**, *61* (52), No. e202212005.
(54) Xu, D.; Huang, S.; Hu, F.; Peng, L.; Jia, S.; Mao, H.; Gong, X.; Li, F.; Qin, W.; Yan, H. Diversity-Oriented Enantioselective Construction of Atropisomeric Heterobiaryls and N-Aryl Indoles via Vinylidene Ortho-Quinone Methides. *CCS Chem.* **2022**, *4* (8), 2686−2697.
(55) Luc, A.; Oliveira, J. C. A.; Boos, P.; Jacob, N.; Ackermann, L.; Wencel-Delord, J. Double cobalt-catalyzed atroposelective C-H activation: One-step synthesis of atropisomeric indoles bearing vicinal C-C and C-N diaxes. *Chem. Catal.* **2023**, *3* (10), 100765.
(56) Wang, B.-J.; Xu, G. X.; Huang, Z. W.; Wu, X.; Hong, X.; Yao, Q. J.; Shi, B. F. Single-Step Synthesis of Atropisomers with Vicinal C−C and C−N Diaxes by Cobalt-Catalyzed Atroposelective C−H Annulation. *Angew. Chem., Int. Ed.* **2022**, *61* (39), No. e202208912.
(57) Gao, Q.; Wu, C.; Deng, S.; Li, L.; Liu, Z. S.; Hua, Y.; Ye, J.; Liu, C.; Cheng, H. G.; Cong, H.; Jiao, Y.; Zhou, Q. Catalytic Synthesis of Atropisomeric o-Terphenyls with 1,2-Diaxes via Axial-to-Axial Diastereoinduction. *J. Am. Chem. Soc.* **2021**, *143* (19), 7253−7260.
(58) Moser, D.; Sparr, C. Synthesis of Atropisomeric Two-Axis Systems by the Catalyst-Controlled syn- and anti-Selective Arene-Forming Aldol Condensation. *Angew. Chem., Int. Ed.* **2022**, *61*, No. e202202548.
(59) Zhan, G.; Du, W.; Chen, Y.-C. Switchable divergent asymmetric synthesis via organocatalysis. *Chem. Soc. Rev.* **2017**, *46* (6), 1675−1692.
(60) Beletskaya, I. P.; Nájera, C.; Yus, M. Stereodivergent Catalysis. *Chem. Rev.* **2018**, *118* (10), 5080−5200.
(61) Kalita, S. J.; Huang, Y.-Y.; Schneider, U. Stereodivergent catalytic asymmetric allylic alkylation (AAA). *Sci. Bull.* **2020**, *65* (22), 1865−1868.
(62) Huo, X.; Li, G.; Wang, X.; Zhang, W. Bimetallic Catalysis in Stereodivergent Synthesis. *Angew. Chem., Int. Ed.* **2022**, *61* (45), No. e202210086.
(63) Moser, D.; Schmidt, T. A.; Sparr, C. Diastereodivergent Catalysis. *JACS Au* **2023**, *3* (10), 2612−2630.
(64) Han, T.-J.; Guan, C.-Y.; Li, N.; Dong, R.; Xu, L.-P.; Xiao, X.; Wang, M.-C.; Mei, G.-J. Catalytic atroposelective synthesis of heterobiaryls with vicinal C−C and N−N diaxes via dynamic kinetic resolution. *iScience* **2023**, *26* (10), 107978.
(65) Han, T.-J.; Zhang, Z. X.; Wang, M. C.; Xu, L. P.; Mei, G.-J. The Rational Design and Atroposelective Synthesis of Axially Chiral C2-Arylpyrrole-Derived Amino Alcohols. *Angew. Chem., Int. Ed.* **2022**, *61* (36), No. e202207517.
(66) Mei, G.-J.; Wong, J. J.; Zheng, W.; Nangia, A. A.; Houk, K. N.; Lu, Y. Rational design and atroposelective synthesis of N−N axially chiral compounds. *Chem* **2021**, *7* (10), 2743−2757.
(67) Dehli, J. R.; Gotor, V. Parallel kinetic resolution of racemic mixtures: a new strategy for the preparation of enantiopure compounds? *Chem. Soc. Rev.* **2002**, *31* (6), 365−370.
(68) Miller, L. C.; Sarpong, R. Divergent reactions on racemic mixtures. *Chem. Soc. Rev.* **2011**, *40* (9), 4550−4562.
(69) Kreituss, I.; Bode, J. W. Flow chemistry and polymer-supported pseudoenantiomeric acylating agents enable parallel kinetic resolution of chiral saturated N-heterocycles. *Nat. Chem.* **2017**, *9* (5), 446−452.
(70) Hilpert, L. J.; Breit, B. Rhodium-Catalyzed Parallel Kinetic Resolution of Racemic Internal Allenes Towards Enantiopure Allylic 1,3-Diketones. *Angew. Chem., Int. Ed.* **2019**, *58* (29), 9939−9943.
(71) De Jesús Cruz, P.; Crawford, E. T.; Liu, S.; Johnson, J. S. Stereodivergent Nucleophilic Additions to Racemic β-Oxo Acid Derivatives: Fast Addition Outcompetes Stereoconvergence in the Archetypal Configurationally Unstable Electrophile. *J. Am. Chem. Soc.* **2021**, *143* (39), 16264−16273.
(72) Wang, X.; Luo, Y.; Li, J.; Wang, C.; Liu, Q.; He, Y.; Luo, S.; Zhu, Q. Parallel Kinetic Resolution through Palladium-Catalyzed Enantioselective Cycloimidoylation: En Route to Divergent N-Heterocycles Bearing a Quaternary Stereogenic Center. *ACS Catal.* **2022**, *12* (24), 14918−14925.
(73) Liu, J.; Du, Y. Y.; He, Y. S.; Liang, Y.; Liu, S. Z.; Li, Y. Y.; Cao, Y. M. Parallel kinetic resolution of aziridines via chiral phosphoric acid-catalyzed apparent hydrolytic ring-opening. *Chem. Sci.* **2023**, *14* (43), 12152−12159.

https://doi.org/10.1021/jacsau.4c00777
JACS Au 2024, 4, 4445−4454

(74) Zhao, K.; Yang, Z.; Yang, J.; Li, X.; Quintanilla, C. D.; Zhang, L. Desymmetrization and Parallel Kinetic Resolution of 1-Ethynylcyclobutanols via Asymmetric Cooperative Gold Catalysis. *J. Am. Chem. Soc.* **2023**, *145* (50), 27205−27210.
(75) Gao, Z.; Yan, C.-X.; Qian, J.; Yang, H.; Zhou, P.; Zhang, J.; Jiang, G. Enantioselective Synthesis of Axially Chiral Sulfonamides via Atroposelective Hydroamination of Allenes. *ACS Catal.* **2021**, *11*, 6931−6938.
(76) Li, S. L.; Yang, C.; Wu, Q.; Zheng, H. L.; Li, X.; Cheng, J. P. Atroposelective Catalytic Asymmetric Allylic Alkylation Reaction for Axially Chiral Anilides with Achiral Morita-Baylis-Hillman Carbonates. *J. Am. Chem. Soc.* **2018**, *140* (40), 12836−12843.
(77) Wang, J.; Gu, J.; Zou, J.-Y.; Zhang, M.-J.; Shen, R.; Ye, Z.; Xu, P.-X.; He, Y. Photocatalytic Z/E isomerization unlocking the stereodivergent construction of axially chiral alkene frameworks. *Nat. Commun.* **2024**, *15* (1), 3254.
(78) The absolute configuration of compound (*R,S*)-**3z** was assigned based on X-ray crystallographic analysis (CCDC 2298809)

https://doi.org/10.1021/jacsau.4c00777
JACS Au 2024, 4, 4445−4454